

Methods for generating propagating shear waves within the heart using MR Elastography

A. Kolipaka¹, K. P. McGee¹, P. A. Araoz¹, and R. L. Ehman¹

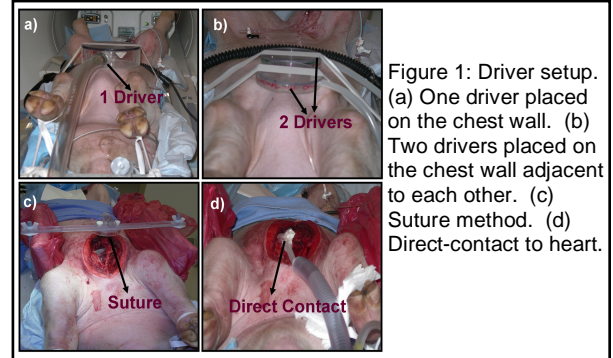
¹Department of Radiology, Mayo Clinic, Rochester, Minnesota, United States

Introduction:

It has been suggested that the intrinsic mechanical properties of the myocardium are directly associated with numerous cardiac disease processes such as diastolic dysfunction, infarction and hypertension [1-3]. One method to quantitate myocardial mechanics would be to spatially resolve the shear modulus of the myocardium using a MR-based technique known as magnetic resonance elastography (MRE) [4]. However a challenge of this novel technique is the introduction of mechanical motion throughout the heart. The aim of this work was to evaluate several noninvasive methods for introducing mechanical motion within the myocardium and to compare them with more invasive methods in an in vivo porcine model.

Methods:

Experimental Setup: In vivo cardiac MRE was performed in six porcine animal models in compliance with our institutional animal care and use committee. The animals were anesthetized by intramuscular injections of a combination of Telazol (5mg/kg), Xylazine (2mg/kg) and Glycopyrrolate (0.06mg/kg) and was also maintained using an isoflurane inhalation anesthesia (1-3%) and were externally ventilated. **Image Acquisition and Analysis:** All imaging was performed in a 1.5-Tesla MRI scanner (Signa Excite, GE Health Care, Milwaukee, WI). With the animal in the supine position and feet first into the scanner, a cine gradient echo MRE sequence was used to acquire multiple phases of the cardiac cycle [5]. Mechanical waves were introduced into the heart by (figure 1): a) **1 Driver:** One large pneumatic drum on the chest wall, b) **2 Drivers:** Two small pneumatic drums adjacent to each other on the chest wall driven in phase and out of phase, c) **Suture:** Opening the chest wall and suturing a thread directly to the apex of the left ventricle (LV) and connecting the other end of the thread to a pneumatic



driver, d) **Direct Contact:** Small pneumatic drum directly on the heart within a closed chest. A 2-chamber long and short-axis slice at the midventricular level were chosen for MRE to avoid the papillary muscles. Imaging parameters included TE/TR= 11.7/25 ms, FOV= 26-27 cm, $\alpha = 30^\circ$, slice thickness= 5 mm; acquisition matrix= 256x64; receiver bandwidth= ± 16 kHz; excitation frequency= 80 Hz; heart rate= 63-143 bpm; views per segment= 4; 4 MRE time offsets; and 6.25-ms duration (160 Hz) MEGs applied separately in the x, y and z directions. Images were acquired at end-systolic and end-diastolic phases of the cardiac cycle for both the long-axis and short-axis slices. Additionally, 20 cardiac phases of the short-axis slice were also reconstructed. The wave images were then processed to obtain the amplitude of the first harmonic of displacement. The mean value of the amplitude from both slices for all sensitization directions were calculated for each pig. The mean of the root mean square (RMS) amplitude of all 3 directions for all six porcine heart models was then calculated and compared between the different driver setups.

Results:

Figure 2(a-f) shows an example of waves induced in the heart using the 2-drivers system when driven out of phase for long- and short-axis slices for all three sensitization directions at end-diastole. The corresponding first harmonic amplitudes are shown in figure 3(a-f). Figure 4(a-d) shows the mean RMS amplitude in the long and short-axis slices at end-systole and end-diastole for all sensitizing directions for all porcine hearts. Figure 4 (e) shows the mean RMS amplitude for all sensitization directions for the short-axis slice for all 6 data sets using the 1-driver system throughout the cardiac cycle (i.e. from end-systole to end-systole, where end-diastole is around the 10th cardiac phase, and the end-systolic phases are represented by the 1st and 20th cardiac phases).

Discussion:

The above results indicate that there is no significant difference in mean RMS amplitude between the end-diastolic and end-systolic phases using any of the driver setups. Amplitude differences between the drivers during end-systole and end-diastole are because of varying contact area of drivers with the body. We have also observed that the mean RMS amplitudes obtained in the long-axis were slightly higher than the short-axis. These results indicate that shear waves can be readily induced and visualized in the heart noninvasively using a pneumatic drum driver.

References:

1. Zile, M.R, et al, Circulation, 2002.105(11):1387-93.
2. Pislaru, C.J, et al, Circulation, 2004.109(23):2905-10.
3. Badenhorst, D, et al, Cardiovas. Research, 2003.57(3):632-41.
4. Muthupillai, R, et al, Science, 1995;269:1854-1857
5. Polzin, J.A, et al, Magn Reson Med, 1996;35(5):755-762.

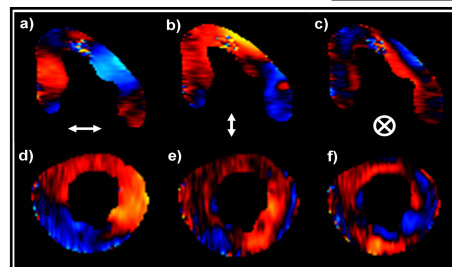


Figure 2: Horizontal, vertical, and through-plane components of displacement for one offset, for a long (a-c) and short-axis slice (d-f) during end-diastole using the 2-drivers setup driving out of phase.

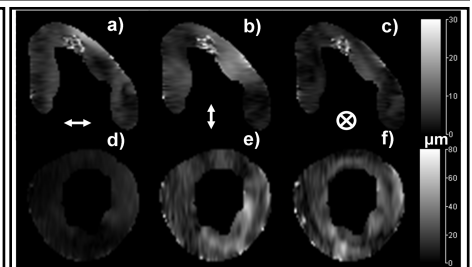


Figure 3: The displacement amplitude maps for the horizontal, vertical, and through-plane components of motion, respectively, for the long (a-c) and short-axis slice (d-f) corresponding to figure 2.

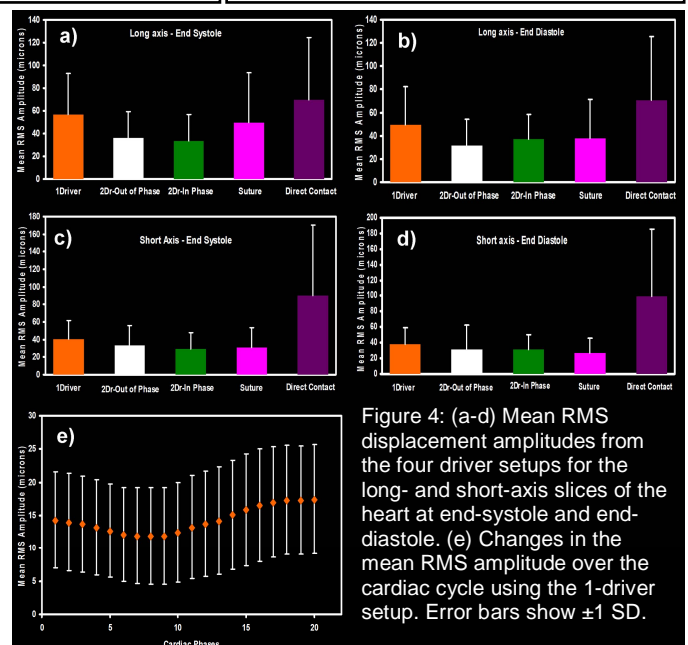


Figure 4: (a-d) Mean RMS displacement amplitudes from the four driver setups for the long- and short-axis slices of the heart at end-systole and end-diastole. (e) Changes in the mean RMS amplitude over the cardiac cycle using the 1-driver setup. Error bars show ± 1 SD.